Ferromagnetic resonance and magnetic precessions in φ_0 junctions

Yu. M. Shukrinov,[1,2] I. R. Rahmonov,[1,3] and K. Sengupta[4]
[1]*BLTP, Joint Institute for Nuclear Research, Dubna, Moscow Region 141980, Russia*
[2]*Department of Nanotechnology and New Materials, Dubna State University, Dubna 141980, Russia*
[3]*Umarov Physical Technical Institute, TAS, Dushanbe 734063, Tajikistan*
[4]*School of Physical Sciences, Indian Association for the Cultivation of Science, Jadavpur, Kolkata 700032, India*

(Received 12 November 2018; revised manuscript received 4 June 2019; published 26 June 2019)

We show that a current sweep along the IV curve of the φ_0 junction may lead to regular magnetization dynamics with a series of specific phase trajectories. The origin of these trajectories is related to a direct coupling between the magnetic moment and the Josephson oscillations in these junctions and ferromagnetic resonance when Josephson frequency coincides with the ferromagnetic one. We demonstrate that an external electromagnetic field can control the dynamics of magnetic moment within a current interval corresponding to a Shapiro step and produce a specific transformation of precession trajectories. As an effect of the coupling between magnetization and spin-orbit interaction, we demonstrate the appearance of the dc component of superconducting current and clarify its role in the transformation of IV characteristics in the resonance region. Good agreement between numerical and analytical results has been found in the ferromagnetic resonance region. The presented results might be used for developing novel resonance methods of determination of the spin-orbit coupling parameter in noncentrosymmetric materials. We discuss experiments which can test our results.

DOI: 10.1103/PhysRevB.99.224513

I. INTRODUCTION

Superconducting spintronics is one of the intensively developing fields of condensed-matter physics today. An important place in this field is occupied by the investigations of Josephson junctions (JJs) coupled to magnetic systems [1,2]. The ability to manipulate the magnetic properties by Josephson current and its opposite, i.e., to influence the Josephson current by the magnetic moment, has attracted a great deal of recent attention [3–6]. The central role in these phenomena is played by spin-orbit interaction. In superconductor/ferromagnet/superconductor (S/F/S) Josephson junctions, the spin-orbit interaction in a ferromagnet without inversion symmetry provides a mechanism for a direct (linear) coupling between the magnetic moment and the superconducting current. Such noncentrosymmetric ferromagnetic junctions, hereafter called φ_0 junctions, break time-reversal symmetry. Consequently, the current-phase relation (CPR) of these junctions is given by $I = I_c \sin(\varphi - \varphi_0)$, where the phase shift φ_0 is proportional to the magnetic moment perpendicular to the gradient of the asymmetric spin-orbit potential [7].

Josephson φ_0 junctions with the current-phase relation $I = I_c \sin(\varphi - \varphi_0)$, where the phase shift φ_0 is proportional to the magnetic moment perpendicular to the gradient of the asymmetric spin-orbit potential, demonstrate a number of unique features important for superconducting spintronics and modern informational technologies. This feature of the CPR allows one to manipulate the internal magnetic moment using the Josephson current [7,8]. In a φ_0 junction the magnetization is coupled to the spin-orbit effect. Thus, once the magnetization rotates, a reverse phenomenon should be expected. Namely, it might pump current through the φ_0 phase shift which is fueled by the term proportional to magnetization and spin-orbit coupling. As we demonstrate below, it leads to the appearance of the dc component of the superconducting current, and we clarify its role in the transformation of IV characteristics in the resonance region.

The theory of the anomalous Zeeman effect and spin-galvanic effect in φ_0 junctions was discussed in Refs. [9,10]. Experimental realization of the φ_0 junction was recently reported by Szombati *et al.* [11]. In Ref. [12], the authors argued that the φ_0 Josephson junction is ideally suited for studying quantum tunneling of the magnetic moment. They proposed that magnetic tunneling would show up in the ac voltage across the junction and it could be controlled by the bias current applied to the junction.

The anomalous Josephson effect in different hybrid heterostructures reflects the interplay of superconductivity, spin-orbit interactions, and magnetism at the same time [13–28]. The investigation of such heterostructures that combine superconducting and ferromagnetic elements gives insight into the problem of the mutual influence of superconductivity and ferromagnetism, allows a realization of exotic superconducting states such as the Larkin-Ovchinnikov-Fulde-Ferrell state and triplet ordering, and promises applications that utilize the spin degree of freedom [19]. The possibility of the anomalous Josephson effect in Supercunductor/Normal Metal/Supercunductor (SNS) junctions can be expected where the normal region is a heterostructure formed by alternating ferromagnetic and spin-orbit coupled segments. It is also shown that a sizable direction dependency of the critical current can be observed in the experiments [14].

The interplay of Rashba and Zeeman interactions in a one-dimensional quantum wire gives rise to an anomalous phase shift in the current-phase relation for the supercurrent [15].

As demonstrated in Ref. [15], the resonance effects which are significant for transport properties of weakly interacting electrons in symmetric junctions survive in the presence of a strong Rashba interaction only for special boundary conditions at normal-metal/superconductor interfaces. With an in-plane external magnetic field an anomalous supercurrent appears even for zero phase difference between the superconducting electrodes [16]. The external field induces large critical current asymmetries between the two flow directions, leading to supercurrent rectifying effects.

Several interesting features may appear if one takes into account the surface of the Josephson junction. Particularly, it was demonstrated in Ref. [21] that its ground state corresponds to the phase difference $\pi/2$ in a superconductor-ferromagnet-superconductor Josephson junction with a critical current density that has a random sign along the junction's surface. A supercurrent 0-π crossover as a function of junction thickness, magnetization strength, and parameters inherent to the helical modulation and surface states is found in a Josephson junction made of disordered surface states of a three-dimensional topological insulator with a proximity-induced in-plane helical magnetization [21]. A generic nonaligned Josephson junction in the presence of an external magnetic field reveals an unusual flux-dependent current-phase relation [26]. Such nonaligned Josephson junctions can be utilized to obtain a ground state other than zero and π, corresponding to the φ junction, which is tunable via the external magnetic flux. A tunable $\pm\varphi$ and hybrid system between the φ and φ_0 junctions were investigated in Refs. [23–25].

Interesting features are observed in Josephson junctions composed of two semiconducting nanowires with Rashba spin-orbit coupling and induced superconductivity from the proximity effect [28]. A 4π-periodic Josephson effect due to the combination of fermion parity conservation and the presence of a topologically protected odd number of zero-energy crossings in the Andreev spectrum is a signature of Majorana zero modes and topological superconductivity. It is shown that for certain orientations of the external magnetic field, such junctions possess a chiral symmetry which allows the existence of the Andreev spectrum. The junction displays a geometrically induced anomalous Josephson effect, the flow of a supercurrent in the absence of external phase bias [28].

Although the static properties of the S/F/S structures are well studied both theoretically and experimentally, much less is known about the magnetic dynamics of these systems [29–31]. Recently, the presence of an anomalous phase shift of φ_0 was experimentally observed directly through CPR measurement in a hybrid SNS JJ fabricated using Bi_2Se_3 (which is a topological insulator with strong spin-orbit coupling) in the presence of an in-plane magnetic field [32]. This constitutes a direct experimental measurement of the spin-orbit coupling strength and opens up new possibilities for phase-controlled Josephson devices made from materials with strong spin-orbit coupling.

It was demonstrated that the dc superconducting current applied to a S/F/S φ_0 junction might produce a strong orientation effect on the ferromagnetic layered magnetic moment [33]. The application of dc voltage to the φ_0 junction would produce current oscillations and consequently magnetic precession. As shown in Ref. [8], this precession may be monitored by the appearance of higher harmonics in the CPR as well as by the presence of a dc component of the superconducting current that increases substantially near the ferromagnetic resonance (FMR). The authors stressed that the magnetic dynamics of the S/F/S φ_0 junction may be quite complicated and strongly anharmonic. In contrast to these results, we demonstrate here that precession of the magnetic moment in some current intervals along the IV curve may be very simple and harmonic. It is expected that external radiation will lead to a series of novel phenomena. Out of this, the possibility of the appearance of half-integer Shapiro steps (in addition to the conventional integer steps) and the generation of an additional magnetic precession with the frequency of external radiation was already discussed in Ref. [8]. However, to the best of our knowledge, an important problem related to the reciprocal influence of the Josephson current and magnetization at different bias currents along the current-voltage (IV) curve has not been investigated until now. Furthermore, the variation of the magnetic precessions in the φ_0 junction along the IV curve has not also been addressed.

In this paper, we present the results on the magnetic precession in φ_0 junctions with a current sweep along the IV curve. This allows us to find specific current intervals with very simple magnetization dynamics. We show that the origin of these trajectories is related to direct coupling between the magnetic moment and the Josephson oscillations, realized in these junctions, and the manifestation of ferromagnetic resonance features when the Josephson frequency is close to the ferromagnetic one. We also demonstrate that the interaction of the Josephson current and the magnetic moment manifests several interesting features under external electromagnetic radiation. In particular, the external radiation can tune the nature of magnetic moment precession in a current interval corresponding to the Shapiro step. We show that such external radiation can produce a specific transformation of magnetization precession trajectories. We numerically demonstrate the appearance of the dc component of the superconducting current and clarify its role in the transformation of IV characteristics in the resonance region. The effects of Gilbert damping and spin-orbit coupling on IV characteristics, magnetization precession, and ferromagnetic resonance features are clarified.

II. MODEL AND METHOD

In Josephson junctions with a thin ferromagnetic layer the superconducting phase difference and magnetization of the F layer are two coupled dynamical variables. The system of equations describing the dynamics of these variables is obtained from the Landau-Lifshitz-Gilbert (LLG) equation and Josephson relations for current and phase difference. Particularly, the magnetization dynamics of our system is described by the Landau-Lifshitz-Gilbert equation where the effective field depends on the phase difference,

$$\frac{d\mathbf{M}}{dt} = -\gamma \mathbf{M} \times \mathbf{H}_{\mathbf{eff}} + \frac{\alpha}{M_0}\left(\mathbf{M} \times \frac{d\mathbf{M}}{dt}\right),$$
$$\mathbf{H}_{\mathbf{eff}} = \frac{K}{M_0}\left[Gr \sin\left(\varphi - r\frac{M_y}{M_0}\right)\widehat{\mathbf{y}} + \frac{M_z}{M_0}\widehat{\mathbf{z}}\right], \qquad (1)$$

where γ is the gyromagnetic ratio, α is a phenomenological damping constant, φ is the phase difference between the superconductors across the junction, $M_0 = \|\mathbf{M}\|$, $G = E_J/(K\mathcal{V})$, K is an anisotropic constant, $\mathcal{V}$ is the volume of the ferromagnetic F layer, $r = l\upsilon_{so}/\upsilon_F$ is a parameter of spin-orbit coupling, υ_{so}/υ_F characterizes the relative strength of the spin-orbit interaction, υ_F is Fermi velocity, $l = 4hL/\hbar\upsilon_F$, L is the length of the F layer, and h denotes the exchange field in the ferromagnetic layer. To follow the estimations in Ref. [10], for parameter r, which is determined by the strength of the spin-orbit interaction and exchange field, we use the values 0.05, 0.5, and 1 in our calculations.

Based on the equations for JJs and the magnetic system, we can rewrite the total system of equations (to be used in our numerical studies) in normalized units

$$\begin{aligned}
\dot{m}_x &= \frac{\omega_F}{1+\alpha^2}\big\{ - m_y m_z + Grm_z \sin(\varphi - rm_y) \\
&\quad - \alpha\big[m_x m_z^2 + Grm_x m_y \sin(\varphi - rm_y)\big]\big\}, \\
\dot{m}_y &= \frac{\omega_F}{1+\alpha^2}\big\{m_x m_z \\
&\quad - \alpha\big[m_y m_z^2 - Gr\big(m_z^2 + m_x^2\big)\sin(\varphi - rm_y)\big]\big\}, \qquad (2) \\
\dot{m}_z &= \frac{\omega_F}{1+\alpha^2}\big\{ - Grm_x \sin(\varphi - rm_y) \\
&\quad - \alpha\big[Grm_y m_z \sin(\varphi - rm_y) - m_z\big(m_x^2 + m_y^2\big)\big]\big\}, \\
\frac{dV}{dt} &= \frac{1}{\beta_c}[I - V - \sin(\varphi - rm_y)], \qquad \frac{d\varphi}{dt} = V,
\end{aligned}$$

where $\beta_c = 2eI_cCR^2/\hbar$ is the McCumber parameter, $m_i = M_i/M_0$ for $i = x, y, z$, and $\omega_F = \Omega_F/\omega_c$, with the ferromagnetic resonance frequency $\Omega_F = \gamma K/M_0$ and characteristic frequency $\omega_c = 2eRI_c/\hbar$. Here we normalize time in units of ω_c^{-1}, external current I in units of I_c, and the voltage V in units of $V_c = I_cR$. This system of equations, solved numerically using the fourth-order Runge-Kutta method, yields $m_i(t)$, $V(t)$, and $\varphi(t)$ as a function of the external bias current I. After the averaging procedure [34,35] we can find IV characteristics at fixed system parameters and investigate the dynamics of magnetization along the IV curve [36].

The system of equations (2) is significantly simplified in the absence of dissipation ($\alpha = 0$). It allows us to clearly understand the magnetization dynamics corresponding to the different points of the IV curve. For this purpose we calculate the temporal dependence of V and m_i at small dissipation ($\alpha \ll 1$) for each value of bias current. In parallel, we also verify the dynamics of the magnetic system by solving the LLG equations at some averaged values of voltage, which corresponds to the voltage-biased JJ. In this case we have replaced φ by Vt in the three first equations of the system (2). The results obtained in this case are in qualitative agreement with the solutions of the system (2).

III. MANIFESTATION OF FMR AT SMALL G AND r

When a current smaller than the critical one ($I < I_c$) is applied to the φ_0 junction, the rotation of the magnetic moment M_y is determined by $\sin\theta = (I_s/I_c)Gr$ ($M_y = M\sin\theta$, where θ is the angle between the z axis and the M direction),

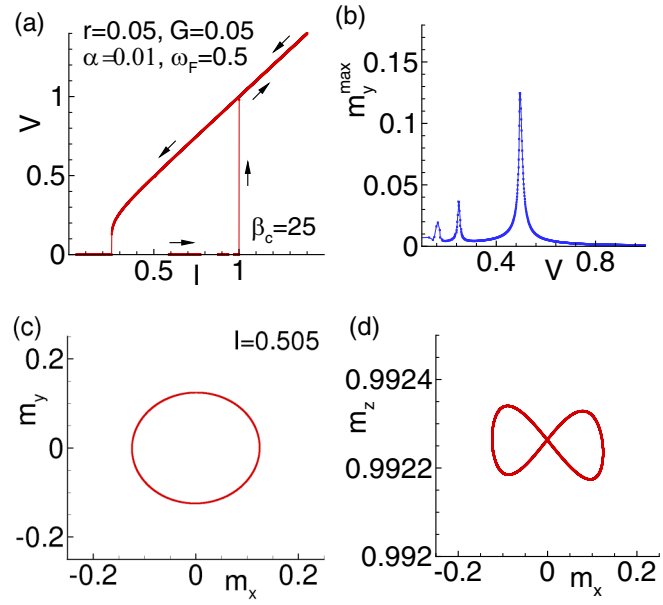

FIG. 1. (a) IV characteristic of the φ_0 junction. (b) Manifestation of the ferromagnetic resonance in the voltage dependence of $m_y^{\max}$. (c) Magnetization trajectory in the m_x-m_y plane at current $I = 0.505$ corresponding to the maximum of the resonance curve in (b); (d) the same in the m_x-m_z plane.

which signifies that the superconducting current provokes the rotation of M in the yz plane [8].

First, we demonstrate the interaction between superconducting current and magnetic moment and show the manifestation of the ferromagnetic resonance in the φ_0 junction. For this purpose we calculate the I dependence of the maximal m_y component at each step of bias current. To see the effect clearly, we make simulations at very small values of the parameters G and r.

In Fig. 1(a), we present the calculated one-loop IV curve (obtained by increasing and decreasing I), which displays an expected hysteresis for $\beta_c = 25$. The IV characteristic for the chosen parameters of the system does not react practically to the changes in the magnetization dynamics. Later, we will discuss this question and show the resonance manifestation in the IV curve at larger r and G. Here we will concentrate on the features near the ferromagnetic resonance which corresponds to the return branch around $\omega_F = V = 0.5$. Figure 1(b) presents the voltage dependence of the maximal amplitude of magnetic moment oscillations $m_y^{\max}$ taken in the time domain at each value of bias current calculated at small values of the Josephson to magnetic energy relation $G = 0.05$ and the parameter of spin-orbit coupling $r = 0.05$. We see the resonance peak around $V = \omega_J = \omega_F = 0.5$ and its two harmonics at $V = \omega_J/2$ and $V = \omega_J/3$, where Josephson frequency is determined as $\omega_J = d\varphi/dt$. The trajectory of magnetization in the m_y-m_x plane at bias current $I = 0.505$ corresponding to the resonance peak is shown in Fig. 1(c). The dynamics of magnetization is very simple here and corresponds to the rotation of the magnetic moment around the z axis. A small deviation to the y axis changes periodically during one rotation circle, so in the m_z-m_x plane the magnetic moment describes the form shown in Fig. 1(d).

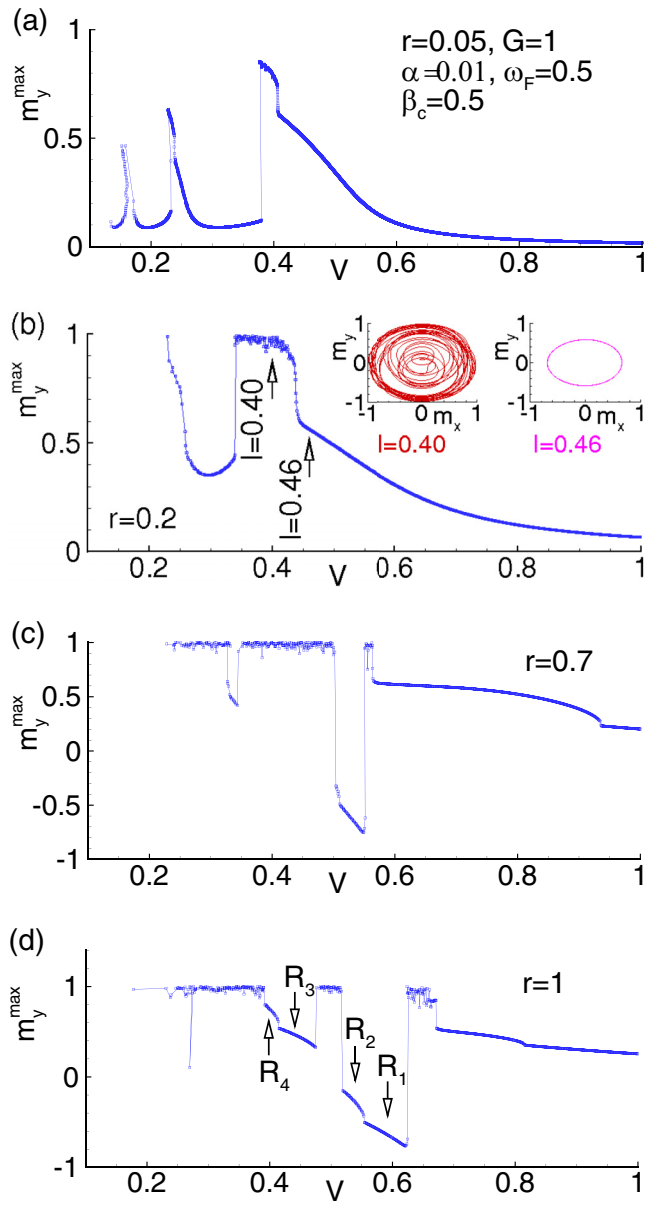

FIG. 2. Transformation of the ferromagnetic resonance region by changing the spin-orbit coupling r. Other parameters are the same and are indicated in (a).

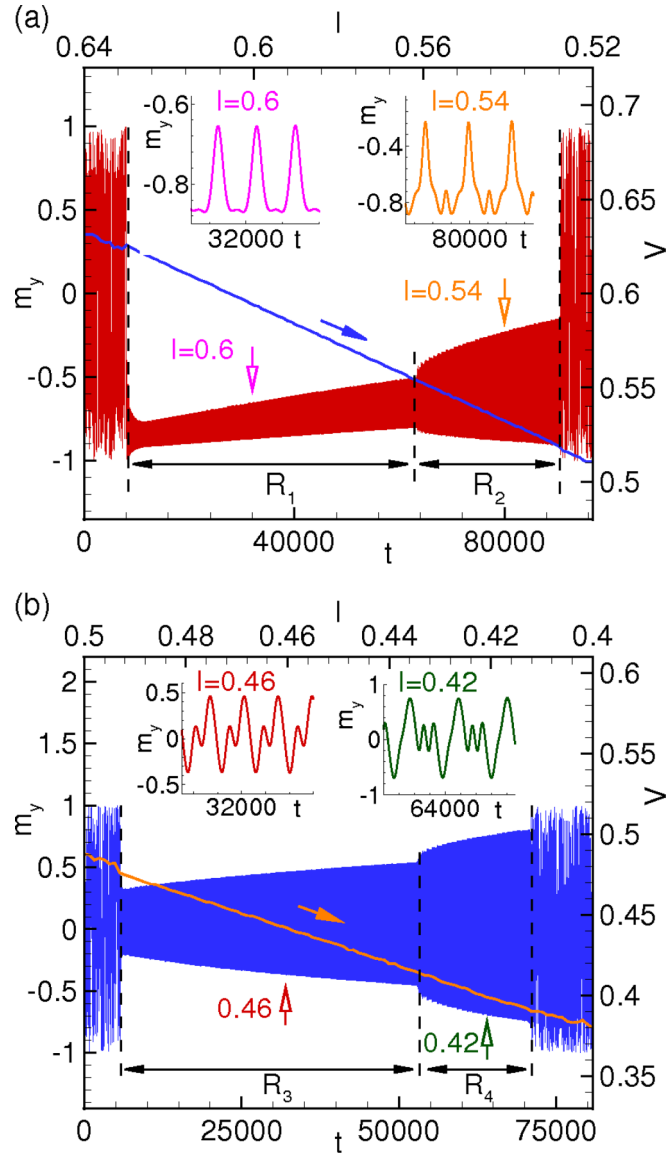

FIG. 3. (a) Time dependence of m_y in the regular region shown by the arrow in Fig. 2(d). Insets demonstrate the character of the $m_y(t)$ oscillations in the R_1 and R_2 current intervals. (b) The same for the second region. The lines show the corresponding parts of IV characteristics.

IV. EFFECT OF SPIN-ORBIT COUPLING

The main ingredient of the considered model is the spin-orbit interaction in the ferromagnetic layer, so it plays a crucial role in the effects discovered in this paper. Figure 2 presents a transformation of voltage dependence of $m_y^{\max}$ by changing the parameter of spin-orbit coupling r. To clarify the effect, we have taken a larger value of the Josephson to magnetic energy of relation G in comparison with the results presented in Fig. 1. With increasing r, the peaks are shifted and widened, reflecting the damped resonance, and their intensity increases. We observe a complex resonance region with different types of magnetization trajectories along the IV curve. Particularly, in the insets of Fig. 2(b) we demonstrate the transformation of trajectories (in the xy plane) with a decrease in bias current at $I = 0.46$ and $I = 0.40$. In Fig. 2(d) we can clearly distinguish the regular regions (R_1, R_2, R_3, and R_4) indicated by arrows. One of the main questions studied in this paper concerns the reaction of the magnetic system to the superconducting current reflected in the appearance of such regular regions. So in what follows, we shall concentrate on the current intervals with regular dynamics.

To clarify the dynamics in the selected regular regions, we have investigated the time dependence of the magnetization component m_y presented in Fig. 3 together with the corresponding parts of the IV curve. Two different parts are clearly pronounced in these regions where the amplitude of m_y grows with decreasing bias current and has a jump between them. These parts are denoted as R_1 and R_2 in the first

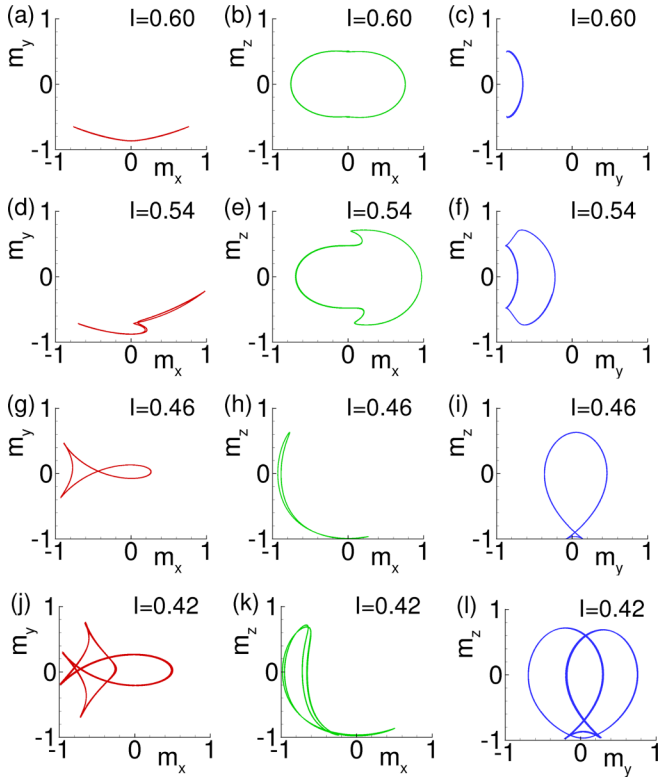

FIG. 4. Magnetization trajectories in the planes m_y-m_x, m_z-m_x, and m_z-m_y for regular regions R_i.

region and R_3 and R_4 in the second one. Demonstrated in the insets, the enlarged time dependence of m_y taken at arbitrary currents shows a different character of oscillations. This fact explains the observed jumps between R_1 and R_2 in the first region and R_3 and R_4 in the second one. As we demonstrate below, the origin of different time dependences in these regions is related to the change of the character of magnetic precessions.

V. SPECIFIC PHASE TRAJECTORIES

Here we demonstrate that current intervals R_i indicated in Figs. 2 and 3 are characterized by different trajectories of the magnetic moment. The characteristic trajectories in the planes m_y-m_x, m_z-m_x, and m_z-m_y realized in these regions are shown in Fig. 4 for four values of bias current $I = 0.60$, 0.54, 0.46, and 0.42. We see different specific forms of trajectories, and some of them for distinctness we call "apple" [Fig. 4(b)], "sickle" [Fig. 4(d)], "mushroom" [Fig. 4(e)], "fish" [Fig. 4(g)], and "moon" [Fig. 4(h)]. The first current interval R_1 is characterized by the apple-type dynamics demonstrated in Fig. 4(b) at $I = 0.60$. With decreasing bias current we observe a transformation of trajectories of apple to mushroom type in the m_z-m_x plane, while the third interval R_3 is characterized by fish- and moon-type trajectories. In the fourth interval R_4 we observe the characteristic trajectory of the "double-fish" type. Thus, the presented results demonstrate a unique possibility of controlling the magnetization dynamics via external bias current.

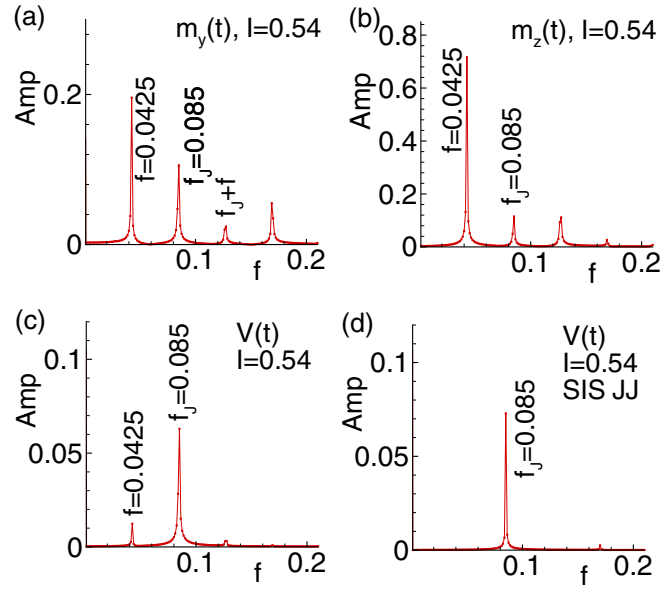

FIG. 5. FFT analysis of time dependencies of (a) $m_y(t)$, (b) $m_z(t)$, (c) $V(t)$, and (d) $V(t)$ for JJs without the magnetic system at $I = 0.54$.

To test whether the observed temporal dependencies of magnetization are related to the Josephson oscillations, we make a detailed fast Fourier transform (FFT) analysis at different values of bias current. In particular, in Fig. 5 we present the results of FFT analysis of the time dependence of the magnetization components and voltage for JJs with and without the magnetic system at $I = 0.54$. Comparing the results presented in Fig. 5, we find that the dynamics of magnetization in this case is really determined by Josephson frequency $f_J = \omega_J/(2\pi) = 0.085$. The existence of half harmonics in this parameter regime indicates that the excitation of magnetic dynamics happens parametrically. We also note the effect of the magnetic oscillations on Josephson current which is manifested as a small peak in the FFT of $V(t)$. This peak is absent for any non-φ_0 Josephson junction such as SNS, S/F/S, bridge, etc., where S indicates superconductor, N is a normal metal, and F is a ferromagnetic layer, as demonstrated in Fig. 5(d). The results of the detailed FFT analysis of dynamics magnetization in the φ_0 junction at different values of bias current will be presented somewhere else [36].

VI. EFFECTS OF EXTERNAL RADIATION

Another important feature of the studied magnetization dynamics concerns the possibility of its control via external electromagnetic radiation. The presence of such a radiation amounts to $I \to I(t) = I + A\sin(\omega t)$ in Eq. (2), where ω is the frequency and A is the amplitude of the external radiation [35]. We find that such an external radiation can control the qualitative nature of the magnetic precession in the current interval corresponding to a Shapiro step. To demonstrate this feature, we show the IV characteristic of the φ_0 junction under external radiation with frequency $\omega = 0.366$ and amplitude $A = 1$ (which demonstrates the corresponding Shapiro step

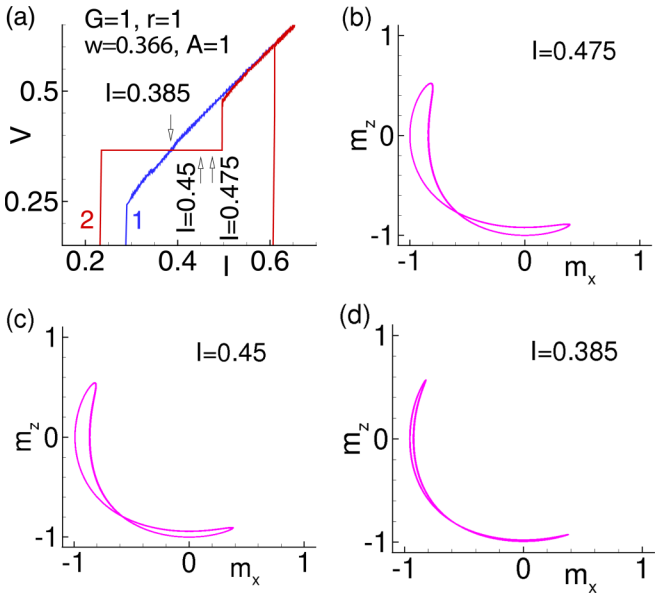

FIG. 6. (a) IV characteristics of JJs without (1) and with (2) radiation. Arrows indicate the bias current values where dynamics of magnetic precessions was investigated. (b) Dynamics of magnetic precession in the m_z-m_x plane in the presence of external radiation at $I = 0.475$. (c) The same at $I = 0.45$. (d) The same at $I = 0.385$.

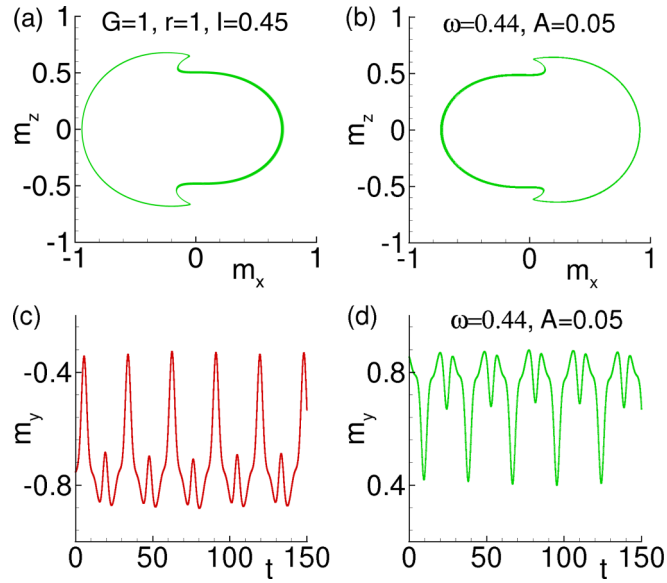

FIG. 7. Left-right transformation by changing the amplitude of external radiation. (a) Dynamics of magnetic precession in the m_z-m_x plane without external radiation at $I = 0.45$. (b) The same under radiation with frequency $\omega = 0.44$ and amplitude $A = 0.05$. (c) Time dependence of m_y without radiation at $I = 0.45$. (d) The same under radiation.

at $V = 0.366$) in Fig. 6(a). The resulting magnetization precessions in the m_z-m_x plane at $I = 0.475$, $I = 0.45$, and $I = 0.385$ are presented in Figs. 6(b), 6(c), and 6(d), respectively. In sharp contrast to magnetization dynamics without radiation (see Fig. 4) demonstrating different specific precession dynamics with changes in bias current, the dynamics of magnetic precessions along the Shapiro step are very similar for all three current values.

Another central result of our work is to demonstrate that the radiation may change the character of magnetic precession. In particular, we show the left-right transformation of mushroom-type precession. As shown in Figs. 7(a) and 7(b), such a change may be accomplished by changing the amplitude of radiation at a fixed dc drive current value $I = 0.45$. This transformation is related to a magnetization reversal from $-m_y$ to $+m_y$, as can be seen from the change in the temporal dependence of $m_y(t)$ in the presence of the external radiation, as demonstrated in Figs. 7(c) and 7(d).

VII. DC CONTRIBUTION TO THE JOSEPHSON CURRENT

As stressed in Refs. [8,36], the Gilbert damping plays an important role in the dynamics of S/F/S JJs. It results in a dc contribution to the Josephson current,

$$I_0(\alpha) = \frac{\alpha G r^2 \omega_J}{4}\left(\frac{1}{\Omega_-} + \frac{1}{\Omega_+}\right), \tag{3}$$

with $\Omega_\pm = (\omega_J \pm 1)^2 + \alpha^2\omega_J^2$. As we see, this contribution depends on the spin-orbit interaction r and relation of Josephson energy to magnetic energy G, and it is absent at $\alpha = 0$.

The result of the superconducting current simulation along IV curves with sweeping the bias current is shown in Fig. 8(a).

Figure 8(a) presents the voltage dependence of $I_s(V)$ together with the analytical curve for I_0, according to (3). We see that in the resonance region the voltage dependence of I_0 is in good agreement with the result for the superconducting current $I_s(V)$. The Gilbert damping leads to the damped

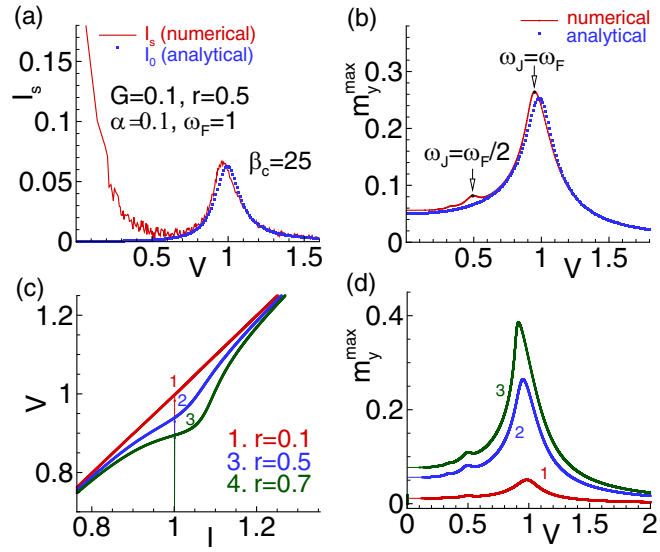

FIG. 8. Demonstration of the ferromagnetic resonance with sweeping bias current along IV characteristics. (a) The voltage dependence of I_s and analytical $I_0(\omega_J)$. (b) The voltage dependence of $m_y^{\max}$ and analytical $m_y(\omega_J)$. (c) The parts of IV characteristics of the φ_0 junction for $G = 0.1$, $r = 0.5$, $\alpha = 0.1$, $\omega_F = 1$ at different values of the spin-orbit interaction. (d) The voltage dependence of $m_y^{\max}$ at different r.

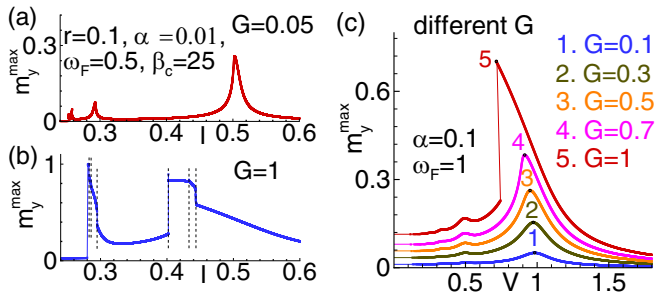

FIG. 9. (a) Dependence of the maximum amplitude of m_y on bias current for the $G = 0.05$ (large anisotropy). (b) The same as (a) for the $G = 1$ (small anisotropy). (c) The voltage dependence of the maximum amplitude of m_y for different values of G.

ferromagnetic resonance at $\omega_J = \omega_F$ with corresponding analytical dependence [8,36] for m_y,

$$m_y(t) = \frac{\omega_+ - \omega_-}{r} \sin \omega_J t - \frac{a_+ + a_-}{r} \cos \omega_J t, \qquad (4)$$

where $\omega_\pm = \frac{Gr^2}{2} \frac{\omega_J \pm 1}{\Omega_\pm}$ and $a_\pm = \frac{Gr^2}{2} \frac{\alpha \omega_J}{\Omega_\pm}$, with $\Omega_\pm = (\omega_J \pm 1)^2 + \alpha^2 \omega_J^2$. In Fig. 8(b), we plot this analytical dependence together with the maximal amplitude $m_y^{\max}$ calculated by the system of equations (2) as a function of voltage. We see good agrement of both results. We stress that numerical calculations do not use any approximations in comparison with analytical ones (where a weak-coupling regime was used considering the case $m_x, m_y \ll 1$), so the simulated dependence reflects additionally the harmonic of the ferromagnetic resonance at $\omega_J = \omega_F/2$.

Based on the presented results, we may note that a variation of the Josephson junction and ferromagnetic layer parameters in the system with damping may lead to a strong enough coupling between the superconducting current and magnetization. Manifestation of such an interaction in the IV characteristic of the φ_0 junction near the ferromagnetic resonance is presented in Fig. 8(c), where we show the parts of the IV characteristics of the φ_0 junction at three values of the spin-orbit interaction at $\omega_F = 1$. The dc contribution to the Josephson current manifests itself as a deviation of the IV curve from the linear dependence in the resonance region. The corresponding voltage dependencies of $m_y^{\max}$ are shown in Fig. 8(d). The effect of the spin-orbit interaction on the resonance character of the presented dependence might form a theoretical background for developing an experimental method for the determination of spin-orbit coupling intensity in the noncentrosymmetric materials.

With the presence of spin-orbit coupling, one can expect anisotropic effects, specifically for the magnetization dynamics. We note that the anisotropic effects are determined by parameter G, which gives the relation between Josephson and magnetic energies. The parameter G was evaluated in Ref. [8] for weak magnetic anisotropy of permalloy, $K \sim 4 \times 10^{-5}$ K Å^{-1} (see Ref. [37]), and a S/F/S junction with $l \sim 1$ and $T_c \sim 10$ K as $G \sim 100$. For stronger anisotropy we may expect $G \sim 1$ or a much smaller value. Figure 9 demonstrates the manifestation of the ferromagnetic resonance features in the current dependence of $m_y^{\max}$. Comparing the results of simulations for $G = 0.05$ in Fig. 9(a) (large anisotropy) with the same in Fig. 9(b) for $G = 1$ (small anisotropy), we see that resonance gets more clearly pronounced at strong anisotropy, but the value of the maximum amplitude of m_y is decreased at the resonance. An important effect of an increase in G (decrease of anisotropy) is a shift of the resonance between Josephson oscillations and magnetic precession, which is shown in Fig. 9(c), where the voltage dependence of the maximum amplitude of m_y for different values of G is demonstrated. This shift is a manifestation of the damped nature of the resonance in agreement with the theoretical results described by formula (3).

VIII. CONCLUSIONS

To summarize, we pointed out an intriguing opportunity to observe a different type of magnetization trajectory by sweeping the current along the IV curves of the φ_0 junction due to a direct coupling between the magnetic moment and the Josephson current. The prediction in Ref. [8] (which is verified in our numerical simulations) that the dc superconducting current in the presence of a constant voltage V applied to the junction implies a dissipative regime can be easily detected experimentally. Good agreement between numerical and analytical results found at the ferromagnetic resonance opens vast opportunities for further manipulation of system parameters and experimental verification of the magnetization dynamics of the materials with strong spin-orbit coupling. This can be easily achieved by applying external radiation to the setup used in Ref. [32].

The appropriate candidate for the experimental verification of the obtained results might be a permalloy doped with Pt [38]. In this material the parameter that characterizes the relative strength of the spin-orbit interaction is $\upsilon_{so}/\upsilon_F \sim 1$. Pt at small doping (up to 10%) did not influence significantly the magnetic properties of permalloy [38], so we may expect υ_{so}/υ_F to reach 0.1 in this case also. If the length of the F layer is of the order of the magnetic decaying length $\hbar/\upsilon_F = h$, i.e., $l \sim 1$, we have $r \sim 0.1$ [33]. Another suitable candidate may be a Pt/Co bilayer, a ferromagnet without inversion symmetry like MnSi, or FeGe. In this material the spin-orbit interaction can generate a φ_0 Josephson junction [7] with a finite ground phase difference. The measurement of this phase difference may serve as an independent way for the parameter r evaluation [11]. As mentioned above, the parameter G for weak magnetic anisotropy of permalloy, $K \sim 4 \times 10^{-5}$ K Å^{-1} (see Ref. [37]), and a S/F/S junction with $l \sim 1$ and $T_c \sim 10K$ can be evaluated as $G \sim 100$. For stronger anisotropy it may be $G \sim 1$ or much smaller. The typical ferromagnetic resonance frequency is $\omega_F = 10$ GHz, which is accessible in the experiments. So we may conclude that our results can be tested experimentally.

A very rich physics is expected if the φ_0 Josephson junction is exposed to microwave radiation. In addition to the features predicted in Ref. [8], particularly, an increase of the Shapiro step amplitude due to spin-orbit coupling near the ferromagnetic resonance, the appearance of the half-integer Shapiro steps, and precession of the magnetization vector with radiation frequency, we expect that an external electromagnetic field can control qualitative features of the magnetic moment dynamics in a current interval which corresponds to

the Shapiro step. Moreover, as we demonstrated in this paper, such radiation can also produce a specific transformation of precession trajectories. We predict that this change in the magnetization dynamics can be observed in such systems as a function of the amplitude of the applied electromagnetic radiation. We consider that the presented results might be used for developing novel experimental resonance methods for the determination of the spin-orbit interaction in noncentrosymmetric materials.

ACKNOWLEDGMENTS

The authors thank A. Mazanik, I. Bobkova, A. Bobkov, and A. Buzdin for helpful discussions. The reported study was partially funded by RFBR research projects 18-02-00318 and 18-52-45011-IND. K.S. thanks DST for support through Indo-Russian Grant No. INT/RUS/RFBR/314. Numerical calculations were made in the framework of RSF project 18-71-10095.

[1] J. Linder and W. A. Jason, Nat. Phys. **11**, 307 (2015).
[2] S. Mai, E. Kandelaki, A. F. Volkov, and K. B. Efetov, Phys. Rev. B **84**, 144519 (2011).
[3] A. I. Buzdin, Rev. Mod. Phys. **77**, 935 (2005).
[4] F. S. Bergeret, A. F. Volkov, and K. B. Efetov, Rev. Mod. Phys. **77**, 1321 (2005).
[5] A. A. Golubov, M. Y. Kupriyanov, and E. Ilichev, Rev. Mod. Phys. **76**, 411 (2004).
[6] R. Ghosh, M. Maiti, Y. M. Shukrinov, and K. Sengupta, Phys. Rev. B **96**, 174517 (2017).
[7] A. Buzdin, Phys. Rev. Lett. **101**, 107005 (2008).
[8] F. Konschelle and A. Buzdin, Phys. Rev. Lett. **102**, 017001 (2009)
[9] F. Dolcini, M. Houzet, and J. S. Meyer, Phys. Rev. B **92**, 035428 (2015).
[10] F. Konschelle, I. V. Tokatly, and F. S. Bergeret, Phys. Rev. B **92**, 125443 (2015).
[11] D. B. Szombati, S. Nadj-Perge, D. Car, S. R. Plissard, E. P. A. M. Bakkers, and L. P. Kouwenhoven, Nat. Phys. **12**, 568 (2016).
[12] E. M. Chudnovsky, Phys. Rev. B **93**, 144422 (2016).
[13] T. Yokoyama, M. Eto, and Y. V. Nazarov, Phys. Rev. B **89**, 195407 (2014).
[14] M. Minutillo, D. Giuliano, P. Lucignano, A. Tagliacozzo, and G. Campagnano, Phys. Rev. B **98**, 144510 (2018).
[15] I. V. Krive, A. M. Kadigrobov, R. I. Shekhter, and M. Jonson, Phys. Rev. B **71**, 214516 (2005).
[16] A. A. Reynoso, G. Usaj, C. A. Balseiro, D. Feinberg, and M. Avignon, Phys. Rev. Lett. **101**, 107001 (2008).
[17] M. Alidoust and H. Hamzehpour, Phys. Rev. B **96**, 165422 (2017).
[18] M. Alidoust, M. Willatzen, and A.-P. Jauho, Phys. Rev. B **98**, 085414 (2018).
[19] V. Braude and Yu. V. Nazarov, Phys. Rev. Lett. **98**, 077003 (2007).
[20] A. Zyuzin, M. Alidoust, and D. Loss, Phys. Rev. B **93**, 214502 (2016).
[21] A. Zyuzin and B. Spivak, Phys. Rev. B **61**, 5902 (2000).
[22] M. Alidoust, Phys. Rev. B **98**, 245418 (2018).
[23] E. Goldobin, D. Koelle, R. Kleiner, and R. G. Mints, Phys. Rev. Lett. **107**, 227001 (2011).
[24] E. Goldobin, D. Koelle, and R. Kleiner, Phys. Rev. B **91**, 214511 (2015).
[25] R. Menditto, M. Merker, M. Siegel, D. Koelle, R. Kleiner, and E. Goldobin, Phys. Rev. B **98**, 024509 (2018).
[26] M. Alidoust and J. Linder, Phys. Rev. B **87**, 060503(R) (2013).
[27] D. S. Shapiro, A. D. Mirlin, and A. Shnirman, Phys. Rev. B **98**, 245405 (2018).
[28] C. Spanslatt, Phys. Rev. B **98**, 054508 (2018).
[29] X. Waintal and P. W. Brouwer, Phys. Rev. B **65**, 054407 (2002).
[30] V. Braude and Ya. M. Blanter, Phys. Rev. Lett. **100**, 207001 (2008).
[31] J. Linder and T. Yokoyama, Phys. Rev. B **83**, 012501 (2011).
[32] A. Assouline, C. Feuillet-Palma, N. Bergeal, T. Zhang, A. Mottaghizadeh, A. Zimmers, E. Lhuillier, M. Eddrie, P. Atkinson, M. Aprili, and H. Aubin, Nat. Commun. **10**, 126 (2019).
[33] Yu. M. Shukrinov, I. R. Rahmonov, K. Sengupta, and A. Buzdin, Appl. Phys. Lett. **110**, 182407 (2017).
[34] Yu. M. Shukrinov, F. Mahfouzi, and N. F. Pedersen, Phys. Rev. B **75**, 104508 (2007).
[35] W. Buckel and R. Kleiner, *Superconductivity: Fundamentals and Application* (Wiley-VCH, Verlag GmbH & Co. KGaA, Weinheim, 2004).
[36] Yu. M. Shukrinov, I. R. Rahmonov, A. A. Mazanik, A. Buzdin, and K. Sengupta (unpublished).
[37] A. Yu. Rusanov, M. Hesselberth, J. Aarts, and A. I. Buzdin, Phys. Rev. Lett. **93**, 057002 (2004).
[38] A. Hrabec, F. J. T. Goncalves, C. S. Spencer, E. Arenholz, A. T. N'Diaye, R. L. Stamps, and C. H. Marrows, Phys. Rev. B **93**, 014432 (2016).